Frequency evaluation of UTC(NPL) by NPL-Sr1 for the period MJD 60614 to 60634

National Physical Laboratory

November 28, 2024

The secondary frequency standard NPL-Sr1 and an optical frequency comb were used to evaluate the frequency of UTC(NPL) over a period of 20 days from MJD 60614 to MJD 60634 (31$^{\text{st}}$ October 2024 – 20$^{\text{th}}$ November 2024). The Sr optical lattice clock operation covers 78.8% of the total measurement period. The result of the evaluation is reported in table 1 and is made using the CCTF 2021 recommended frequency value for the $5s^2\ {}^1S_0$ – $5s5p\ {}^3P_0$ unperturbed optical transition in ^{87}Sr: 429 228 004 229 872.99 Hz with a relative standard uncertainty of $u_{\text{Srep}} = 1.9 \times 10^{-16}$ [1].

Period of estimation	y(UTC(NPL)−NPL-Sr1) $/10^{-16}$	u_{A} $/10^{-16}$	u_{B} $/10^{-16}$	$u_{\text{A/Lab}}$ $/10^{-16}$	$u_{\text{B/Lab}}$ $/10^{-16}$	u_{Srep} $/10^{-16}$	Uptime
MJD 60614–60634	3.60	0.004	0.196	2.09	0.93	1.9	78.8%

Table 1: Results of the evaluation of UTC(NPL) by NPL-Sr1.

1 Measurement configuration

NPL-Sr1 was operated as described in reference [2], with the exception of some changes described in section 2 below. The 698 nm clock laser was pre-stabilized to a local reference cavity and then phase-locked via a fibre-based optical frequency comb to another more stable laser at 1064 nm. A feedback loop acting on an acousto-optic modulator (AOM) kept the clock laser frequency in resonance with the ^{87}Sr clock transition.

Following a change in the reference maser for UTC(NPL) in January 2021, and a subsequent redistribution of reference frequency signals within NPL in February 2021, the optical frequency comb was no longer referenced to UTC(NPL), but instead to a separate maser reference HM6.

The frequency ratio between the ^{87}Sr clock transition and HM6 was calculated from the comb measurements of the 698 nm ultrastable laser and the AOM frequency corrections. The frequency ratio was determined as the midpoint of a weighted linear fit to the NPL-Sr1/HM6 ratio data. The time offset between HM6 and UTC(NPL) was continually measured by an SR620 time interval logger. By taking the derivative of this time offset we determined the mean frequency difference between the two signals over the evaluation period. This was then combined with the frequency comb measurements to obtain the frequency ratio between the ^{87}Sr clock transition and UTC(NPL). HM6 was not steered during this evaluation period.

A second optical frequency comb was used for this evaluation following its installation in October 2024. A comparison of the NPL-Sr1/HM6 ratio data measured by each comb demonstrated a comb agreement of $1.2(1.9) \times 10^{-18}$.

Systematic effect	Correction / 10^{-18}	Uncertainty / 10^{-18}
BBR chamber	5014.4	19.3
BBR oven	0.5	0.5
Quadratic Zeeman	246.2	0.3
Lattice	-6.7	1.3
Collisions	0.4	0.7
Background gas	2.5	0.25
DC Stark	0.016	0.016
Probe Stark	0.0	1.0
Servo Error	0.0	0.0
Total Correction	5257.3	19.4
Gravitational redshift	-1215.0	2.7
Total including gravitational redshift	4042.3	19.6

Table 2: Uncertainty budget for the NPL-Sr1 lattice clock for this evaluation period. Reported uncertainties correspond to 68% confidence intervals. This table applies to the period MJD 60614–60634.

2 NPL-Sr1 evaluation

Type A uncertainty

The type A uncertainty u_A is the statistical contribution from the frequency instability of NPL-Sr1. This was estimated based on a white frequency noise component of $4.5 \times 10^{-16}/\sqrt{\tau}$, extrapolated to the duration of the evaluation period.

This is an improvement compared to the earlier reports covering the periods MJD 58659–58679 ($5 \times 10^{-16}/\sqrt{\tau}$), MJD 58454–58459 ($8 \times 10^{-16}/\sqrt{\tau}$) and MJD 57904–57919 and MJD 57929–57934 ($2 \times 10^{-15}/\sqrt{\tau}$). The improvement is a direct result of improvements made to the 1064 nm laser to which the 698 nm clock laser is stabilised. The stability was evaluated by interleaved measurements.

Type B uncertainty

The type B uncertainty u_B is the sum in quadrature of the systematic uncertainty of NPL-Sr1 and the uncertainty of the gravitational redshift relative to the conventionally adopted reference potential $W_0 = 62\ 636\ 856.0\ \mathrm{m^2 s^{-2}}$.

The systematic frequency corrections and uncertainty budget for NPL-Sr1 for the period of this report are given in table 2. The geopotential value for NPL-Sr1 is taken from [3].

Changes to the uncertainty evaluation presented in reference [2] are described below.

Blackbody radiation

In this report we continue to use the updated dynamic correction coefficient for blackbody radiation, reported in reference [4]. The methodology to evaulate our blackbody radiation correction remains as in [2].

Quadratic Zeeman

For this evaluation, we continued using a nominal stretched state splitting of 640 Hz (similar to that used in reference [2] and in the prior reported periods MJD 60034–60064 and 60064–60079). We continue to use the updated value for the quadratic Zeeman shift coefficient of $-2.456(3)\times10^{-7}$ Hz^{-1} [5].

Background Gas

As for the previous evaluations, we use an updated coefficient for the background gas collisional shift of $(-3.0 \pm 0.3) \times 10^{-17}/\tau$, where τ is the $1/e$ vacuum-limited trap lifetime [6]. Assuming hydrogen is the dominant gas in our system we arrive at a shift of $(-2.50 \pm 0.25) \times 10^{-18}$ based on a lattice trapped lifetime measurement of 12.06 s (re-evaluated after breaking vacuum to perform in-situ radiation thermometry and fixing a small leak in the vacuum system).

Collisions

For this period we have re-evaluated the cold collisional shift through interleaved measurement of high and low atom numbers in a fixed lattice depth. We determine a shift of $(-0.4 \pm 0.7) \times 10^{-18}$ with uncertainty dominated by white frequency noise in the measurement.

Lattice

The same nominal lattice conditions as in the prior reported periods were operated throughout this evaluation period. However, we use an updated weighted mean for the hyperpolarisability coefficient of -458(14) nHz [7], and a coefficient for the multipolar E2 and M1 shift as a weighted mean of experimental values from [7–9] as -949(39) μHz. Following the same method as in [2] we determine the total lattice shift to be $(6.7 \pm 1.3) \times 10^{-18}$.

3 Frequency comparison

Type A uncertainty

The uncertainty $u_{\mathrm{A/Lab}}$ arises mainly from the dead time in the comparison between HM6 and NPL-Sr1, and includes both a deterministic correction due to maser drift and a stochastic contribution (table 3).

The stochastic contribution was estimated by a method described in [10]. This involves a Monte-Carlo approach where the frequency noise of HM6 is simulated and a value calculated for the offset between the mean frequency during the uptime periods and the mean frequency during the whole evaluation period. The simulation was repeated 1000 times, with the standard deviation of the offsets

Contribution	Uncertainty / 10^{-18}
$u_{\mathrm{A/Lab}}$[Deterministic]	25
$u_{\mathrm{A/Lab}}$[Stochastic]	207
$u_{\mathrm{A/Lab}}$[HM6-UTC(NPL)]	16
$\boldsymbol{u_{\mathrm{A/Lab}}}$**[Total]**	209

Table 3: A breakdown of the uncertainties included in $u_{\mathrm{A/Lab}}$.

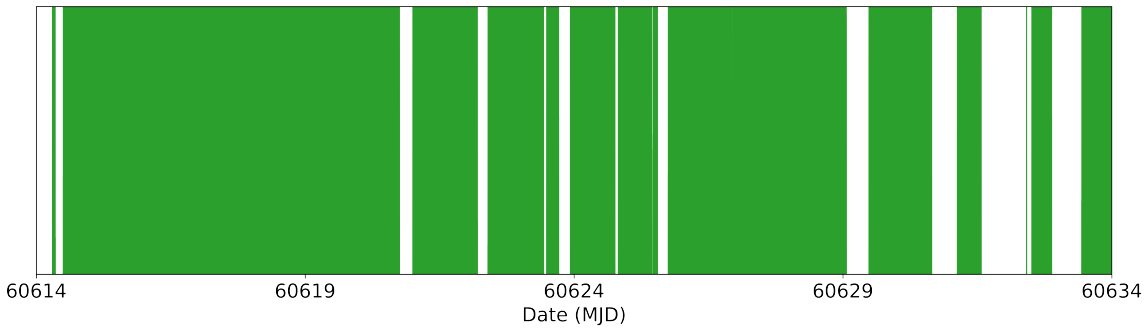

Figure 1: Uptime of NPL-Sr1 over the evaluation period (green regions).

providing an estimate for the frequency uncertainty arising from the dead times in the operation of NPL-Sr1.

The maser noise model used comprised white phase noise of $1.00\times10^{-13}/\tau$, white frequency noise of $5.40\times10^{-14}/\sqrt{\tau}$, a flicker frequency floor of 1.25×10^{-15} and a random-walk frequency component of $2.55\times10^{-19}\sqrt{\tau}$. In addition, maser HM6 exhibits periodic frequency fluctuations that were estimated as an additional noise process proportional to the sum of two sinusoids in the simulated noise, with amplitudes 2.0×10^{-15} and 1.5×10^{-15} and periods 3×10^{4} s and 8.64×10^{4} s respectively. These values were derived from measurements of HM6 by NPL-Sr1 during the evaluation period.

For this evaluation period, NPL-Sr1 had an uptime of 78.8%, distributed as shown in figure 1.

The SR620 time interval logger that links HM6 to UTC(NPL) introduces an additional contribution to $u_{\mathrm{A/Lab}}$, which is computed from the statistical spread of the time interval measurements.

Type B uncertainty

The most significant contribution to the uncertainty $u_{\mathrm{B/Lab}}$ is the distribution of the 10 MHz signal from HM6 to the frequency comb laboratory, and the subsequent synthesis in that laboratory of an 8 GHz signal against which the repetition rate of the frequency comb was measured. Potential phase fluctuations were monitored using a loop-back comparison as described in reference [2], and their contribution to the uncertainty estimated from the instability of these fluctuations over the evaluation period.

The SR620 time interval logger that links HM6 to UTC(NPL) also contributes to $u_{\mathrm{B/Lab}}$. This contribution is estimated based on the specification of the instrument.

Contribution	Uncertainty / 10^{-18}
$u_{\mathrm{B/Lab}}$[Distribution]	83
$u_{\mathrm{B/Lab}}$[HM6-UTC(NPL)]	41
$\boldsymbol{u_{\mathrm{B/Lab}}}$**[Total]**	93

Table 4: A breakdown of the uncertainties included in $u_{\mathrm{B/Lab}}$.

References

[1] Consultative Committee for Time and Frequency (CCTF), "Recommendation PSFS-2 from the 22nd meeting (session II – online)," (2022).

[2] R. Hobson, W. Bowden, A. Vianello, A. Silva, C. F. A. Baynham, H. S. Margolis, P. E. G. Baird, P. Gill, and I. R. Hill, "A strontium optical lattice clock with 1×10^{-17} uncertainty and measurement of its absolute frequency," Metrologia **57**, 065026 (2020).

[3] F. Riedel, A. Al-Masoudi, E. Benkler, S. Dörscher, V. Gerginov, C. Grebing, S. Häfner, N. Huntemann, B. Lipphardt, C. Lisdat, E. Peik, D. Piester, C. Sanner, C. Tamm, S. Weyers, H. Denker, L. Timmen, C. Voigt, D. Calonico, G. Cerretto, G. A. Costanzo, F. Levi, I. Sesia, J. Achkar, J. Guéna, M. Abgrall, D. Rovera, B. Chupin, C. Shi, S. Bilicki, E. Bookjans, J. Lodewyck, R. L. Targat, P. Delva, S. Bize, F. N. Baynes, C. F. A. Baynham, W. Bowden, P. Gill, R. M. Godun, I. R. Hill, R. Hobson, J. M. Jones, S. A. King, P. B. R. Nisbet-Jones, A. Rolland, S. L. Shemar, P. B. Whibberley, and H. S. Margolis, "Direct comparisons of European primary and secondary frequency standards via satellite techniques," Metrologia **57**, 045005 (2020).

[4] C. Lisdat, S. Dörscher, I. Nosske, and U. Sterr, "Blackbody radiation shift in strontium lattice clocks revisited," Phys. Rev. Research **3**, L042036 (2021).

[5] T. Bothwell, D. Kedar, E. Oelker, J. M. Robinson, S. L. Bromley, W. L. Tew, J. Ye, and C. J. Kennedy, "JILA SrI optical lattice clock with uncertainty of 2.0×10^{-18}," Metrologia **56**, 065004 (2019).

[6] B. X. R. Alves, Y. Foucault, G. Vallet, and J. Lodewyck, "Background Gas Collision Frequency Shift on Lattice-Trapped Strontium Atoms," in *2019 Joint Conference of the IEEE International Frequency Control Symposium and European Frequency and Time Forum (EFTF/IFC)* (IEEE, Orlando, FL, USA, 2019) pp. 1–2.

[7] S. Dörscher, J. Klose, S. Maratha Palli, and C. Lisdat, "Experimental determination of the E2–M1 polarizability of the strontium clock transition," Phys. Rev. Research **5**, L012013 (2023).

[8] I. Ushijima, M. Takamoto, and H. Katori, "Operational magic intensity for Sr optical lattice clocks," Phys. Rev. Lett. **121**, 263202 (2018).

[9] P. G. Westergaard, J. Lodewyck, L. Lorini, A. Lecallier, E. A. Burt, M. Zawada, J. Millo, and P. Lemonde, "Lattice-induced frequency shifts in Sr optical lattice clocks at the 10^{-17} level," Phys. Rev. Lett. **106**, 210801 (2011).

[10] D.-H. Yu, M. Weiss, and T. E. Parker, "Uncertainty of a frequency comparison with distributed dead time and measurement interval offset," Metrologia **44**, 91 (2007).